Measurement of the $\bar{p}p \rightarrow \bar{n}n$ Differential Cross Sections at Low Momenta and Confirmation of the Forward Dip

K. Nakamura,[a] T. Fujii, T. Kageyama, F. Sai, S. Sakamoto,[b]
S. Sato,[c] T. Takahashi, T. Tanimori, and S. S. Yamamoto
Department of Physics, University of Tokyo, Tokyo 113, Japan

and

Y. Takada
Institute of Applied Physics, University of Tsukuba, Sakura, Ibaraki 305, Japan
(Received 29 May 1984)

The differential cross sections of the reaction $\bar{p}p \rightarrow \bar{n}n$ were measured at 390, 490, 590, 690, and 780 MeV/c. The existence of the theoretically predicted forward dip is confirmed. The results are compared with the predictions of various $\bar{N}N$ potential models.

PACS numbers: 13.75.Cs, 12.40.Qq

While the low-energy antinucleon-nucleon ($\bar{N}N$) interaction is one of the fundamental problems in nuclear physics, it is not very well understood, unlike the nucleon-nucleon interaction. In particular, the charge-exchange reaction, $\bar{p}p \rightarrow \bar{n}n$, is among the least studied channels despite its importance in determining the detailed structure of the $\bar{N}N$ scattering amplitudes. Although the total charge-exchange cross section has been measured[1] with high statistics below 1 GeV/c, the measurements of the differential cross sections[2] have poor statistics except the one at 700–760 MeV/c by Bogdanski *et al.*[3]

In the one-boson-exchange picture, the pion exchange is the dominant mechanism for $\bar{p}p \rightarrow \bar{n}n$ in the low-momentum-transfer region. It has been argued[4] that the interference of the pion-exchange amplitude and a coherent background amplitude produces a sharp spike followed by a dip-bump structure in the forward direction. The observation of such a structure was reported by Bogdanski *et al.*,[3] and, on the theoretical side, the Bryan-Phillips potential model,[5] although only qualitatively, accounts for this behavior.

We have measured the $\bar{p}p \rightarrow \bar{n}n$ differential cross sections at 390, 490, 590, 690, and 780 MeV/c. In this experiment, we aimed at obtaining high-statistics data which permit detailed comparison with theoretical predictions, as well as confirming the existence of the forward dip in the low-momentum region.

The measurement was performed in a low-momentum separated beam (K3) at the National Laboratory for High Energy Physics (KEK).[6] The experimental arrangement is shown in Fig. 1. A vacuum chamber containing a 17.5-cm-long liquid-hydrogen target was surrounded by a five-layer cylindrical drift chamber (CDC). The target and the CDC were placed in a magnet having 100-cm-diam pole pieces with a 60-cm gap. The applied magnetic field was 2.5 kG at the center. The antiproton beam was defined by the counters C1 (not shown in Fig. 1), C2, and C3, and its trajectory was determined by two multiwire proportional chambers with bidimensional readout and the CDC. Outside of the magnetic field were located four-layer planar drift chambers DC1–DC4. On the surface of the magnet pole pieces were attached scintillation counters (called the pole-face counters, not shown in Fig. 1) in order to detect charged annihilation

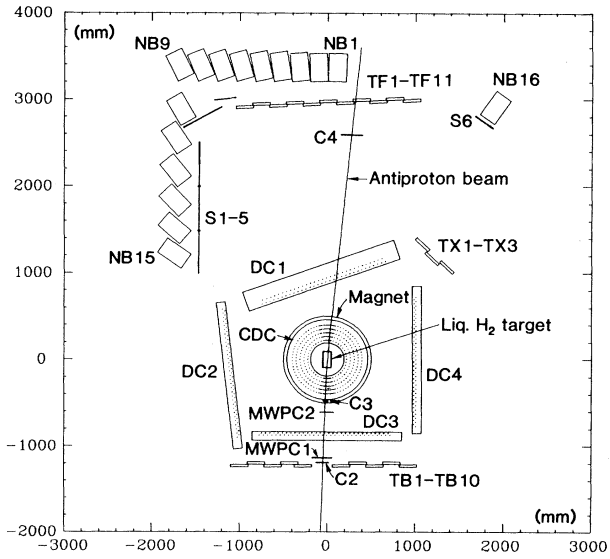

FIG. 1. Experimental arrangement. C2–C4, trigger counters; MWPC1 and MWPC2, multiwire proportional chambers; CDC, cylindrical drift chamber; DC1–DC4, planar drift chambers; TF1–TF11, TB1–TB10, and TX1–TX3, time-of-flight counters; NB1–NB16, iron-scintillator sandwich counters; S1–S6, scintillation counters.

© 1984 The American Physical Society

products. In the forward and backward directions, there were two walls of time-of-flight (TOF) counters, TF and TB. Another TOF counter plane TX was placed to cover the rather large gap between DC1 and DC4.

The antineutrons were detected by iron-scintillator sandwich counters NB. An NB module was 20 cm wide and 80.6 cm high, and consisted of seven layers of 1-cm-thick scintillator interleaved between iron plates with a total thickness of 24.8 cm. Each module was viewed by two photomultipliers located above and below it. Fifteen NB modules were arranged on the left with respect to the beam to measure the antineutron angular distribution. On the opposite side, another module (NB16) was placed in order to study the effect of the neutron background, using the $\bar{p}p \rightarrow \bar{n}n$ events in which the antineutron was detected by NB16 and consequently the neutron hit one of the NB modules on the left according to the two-body kinematics. All NB modules were placed behind scintillation counters (TF or S1–S6).

The events were triggered by $(C1 \cdot C2 \cdot C3)_{\bar{p}}C4$, where $(C1 \cdot C2 \cdot C3)_{\bar{p}}$ represents the incident $\bar{p}$ defined by the counters C1, C2, and C3, and C4 eliminated noninteracting $\bar{p}$ events. This loose trigger requirement was adopted because the intensity of the $\bar{p}$ beam was low (typically 200 $\bar{p}$'s per 10^{12} primary protons at 590 MeV/c) and several reaction channels were concurrently measured. At each beam momentum, events were also taken with a no-bias trigger $(C1 \cdot C2 \cdot C3)_{\bar{p}}$ for the purpose of various checks.

In the analysis, we first examined pulse height and timing of the trigger counters to reduce the contamination of the beam by pions to a level of less than 0.3%. To select the $\bar{p}p \rightarrow \bar{n}n$ candidates we imposed the following criteria: (i) At least one NB module out of NB1–NB15 should have both photomultiplier signals having TDC (time-to-digital converter) information and pulse height of more than 5 ADC (analog-to-digital converter, LRS 2249W) channels above the pedestal; (ii) no charged particle trajectory other than the incident antiproton should exist in the CDC; (iii) there should be no TF, TB, and/or S hits with timing compatible with γ's from π^0's or fast charged pions (missed by the CDC becasue of inefficiency) produced by $\bar{p}p$ annihilation in the target; and (iv) there should be no pole-face-counter hits.

Figure 2(a) shows the summed pulse-height distribution of the two photomultiplier signals of all NB modlules for charged pions and γ's coming from the target, tagged by their fast timing, and that

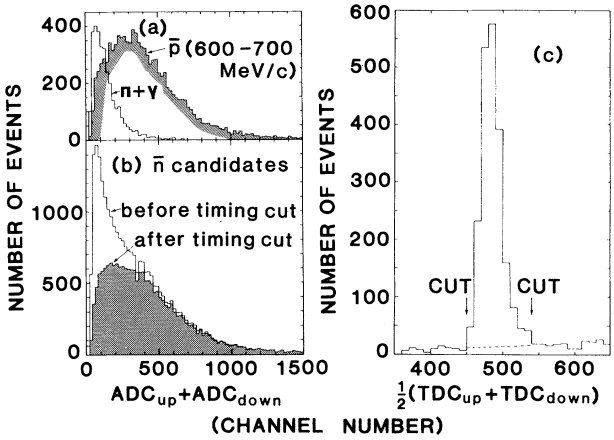

FIG. 2. (a) Summed pulse-height distributions of all NB counter modules for charged pions and gammas coming from the target, and for 600–700-MeV/c antiprotons. (b) Summed pulse-height distributions for all NB counter modules for antineutron candidates at incident $\bar{p}$ momentum of 490 MeV/c. The upper histogram was obtained before the timing cut and the lower shaded histogram was obtained after the timing cut. (c) The timing distribution of NB1 for antineutron candidates at incident $\bar{p}$ momentum of 490 MeV/c. A background level is shown by the dashed line.

for 600–700-MeV/c $\bar{p}$'s. These $\bar{p}$'s can reach the second or third iron layer of the NB module, and therefore their summed pulse-height distribution is considered to be similar to that of $\bar{n}$'s. The summed pulse-height distribution for the $\bar{p}p \rightarrow \bar{n}n$ candidate events is shown by the upper histogram (labeled "before timing cut") in Fig. 2(b). Clearly, these events contain background events with low pulse height. The origin of this background was found to be charged pions or γ's from $\bar{n}$'s annihilated somewhere outside the NB modules (for example, a substantial contribution came from the supporting frame of the NB modules). A timing cut for the NB counter signal as shown in Fig. 2(c) almost eliminated this background. Indeed, after this cut the summed pulse-height distribution, shown by the lower shaded histogram in Fig. 2(b), became similar to that for 600–700 MeV/c $\bar{p}$'s. The residual background under the timing peak [shown by the dashed line in Fig. 2(c)] was later subtracted. If two adjacent modules were hit (30% of the total events), the module with the higher summed pulse height was chosen as the hit module. If two modules not adjacent to each other were hit (3.4% of the total events), the module with the faster timing (within the $\bar{n}$ timing window) was chosen. A Monte Carlo simulation showed that about 87% of the events had correctly assigned hit

modules. Most of the other events had the chosen module adjacent to the hit module. Only less than 1% of the total events had completely wrong hit assignments.

The detection efficiency of the NB module for $\bar{n}$'s depends on the following two factors: (a) *The annihilation probability of $\bar{n}$'s in the NB module.* The absorption length of the $\bar{n}$'s in iron is, for example, 10.1 cm at 500 MeV/c (which is estimated from a recently determined $\bar{p}$-nucleus optical potential[7]), and more than 90% of $\bar{n}$'s annihilate in the NB module. (b) *The energy deposited in the scintillator by the annihilation products (which is called the visible energy).* The event-selection criterion (i) i.e., the requirement of the TDC information, set a lower limit (or a threshold) to the detectable visible-energy distribution. In order to obtain the actual value of the efficiency, the experimental value of this threshold had to be obtained. This was done by use of the measured detection efficiency for $\bar{p}$'s and their Monte Carlo–generated visible-energy distribution. The detection efficiency for $\bar{n}$'s was then determined by use of this threshold and the Monte Carlo–generated visible-energy distribution for $\bar{n}$'s. The resulting NB detection efficiency for $\bar{n}$'s was $1.67p^2+1.5p+72.2\pm4\%$, where p is the $\bar{n}$ momentum in GeV/c. The error includes the module-to-module variation of $\pm2\%$, estimated from the pulse-height distribution for minimum-ionizing particles.

In addition to the $\bar{n}$ detection efficiency, the following corrections were applied. As a result of the event-selection criterion (ii), some $\bar{p}p\rightarrow\bar{n}n$ events were discarded if the incident $\bar{p}$ was accompanied by another charged particle, which caused a correction of $+(7\pm3)\%$. Other corrections are these: the beam absorption by liquid hydrogen, $+(5.3\pm1)-(9.9\pm2)\%$, the absorption by other materials, $+(1\pm1)\%$; the contribution from nontarget materials determined by empty-target runs, $-(3\pm1)\%$; trigger bias due to the requirement of C4, etc., $+(1\pm1)\%$. The total systematic error amounts to $\pm8.5\%$ including the overall normalization uncertainty of $\pm5\%$.

The angular distributions obtained are shown in Figs. 3(a)–3(e). The error bars represent the sta-

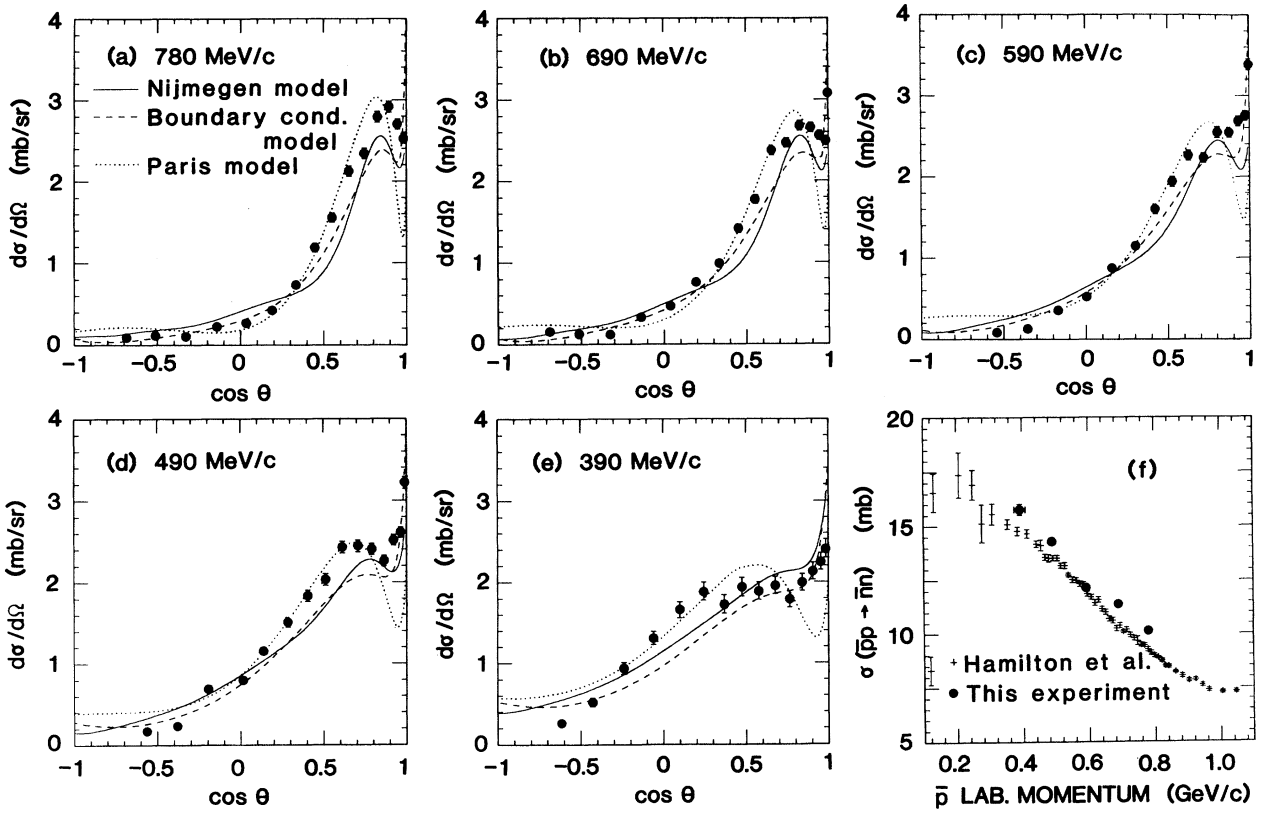

FIG. 3. (a)–(e) The differential cross sections of the $\bar{p}p\rightarrow\bar{n}n$ reaction. The predictions of the Nijmegen model, boundary-condition model, and Paris model are shown by the solid curves, dashed curves, and dotted curves, respectively. (f) The integrated charge-exchange cross-section data are compared with the data of Hamilton *et al.*

tistical errors only. The angular distributions at 390, 490, and 690 MeV/c clearly show the existence of the forward dip. At 590 MeV/c, there is a shoulder instead of a dip due perhaps to statistical fluctuation. At 780 MeV/c, the sharp forward peak is not seen because of the acceptance limitation. (The most forward NB module was not installed in the 780 MeV/c run.) The positions of the dip are $|t| \sim 0.017$, 0.015, and 0.010 at 390, 490, and 690 MeV/c, respectively. At 780 MeV/c, the dip seems to be located at $|t| < 0.01$. These results indicate that the dip moves toward the forward direction with increasing beam momentum.

The integrated charge-exchange cross section is shown in Fig. 3(f) and compared with the data of Hamilton *et al.*[1] The error bars indicate the statistical errors. Our data are somewhat higher than the data of Hamilton *et al.*[1] except at 590 MeV/c. However, considering the systematic errors of $\pm 8.5\%$ for our data and $\pm 5\%$ for the data of Hamilton *et al.*,[1] these data are not inconsistent.

Finally, we have compared the differential cross-section data with the predictions of some $\bar{N}N$ potential models: the boundary-condition model,[8] Paris model,[9] and Nijmegen model.[10] In the boundary-condition–model calculation, the G-parity–transformed Bryan-Scott one-boson-exchange potential[11] was used with the boundary radius of $r_c = 0.5$ fm. The calculated $\bar{p}p \to \bar{n}n$ differential cross sections are shown by the curves in Figs. 3(a)–3(e). All three models predict the existence of the forward dip. The position and depth of the dip seem to be reasonably reproduced by the boundary-condition model[8] and by the Nijmegen model.[10] However, the Paris model[9] shows better agreement with the data except in the dip region. As a matter of fact, none of these models completely explains the behavior of the data. This indicates the necessity for fine-tuning the parameters involved in the models.

In summary, we have presented the $\bar{p}p \to \bar{n}n$ differential cross-section data at incident $\bar{p}$ momenta between 390 and 780 MeV/c. The existence of the forward dip has been confirmed over this momentum range. We are grateful to the staff of the National Laboratory for High Energy Physics for excellent machine operation and technical assistance. We wish to thank Dr. T. Mizutani, Dr. M. Lacombe, and Dr. P. Timmers for sending us their results of calculation with $\bar{N}N$ potential models. Thanks are also due to Mr. Y. Umeda who participated in the early phase of this experiment.

[a]Present address: National Laboratory for High Energy Physics, Oho, Ibaraki 305, Japan.

[b]Present address: Rutherford-Appleton Laboratory, Chilton, Didcot, Oxon, United Kingdom.

[c]Present address: Computer Engineering Division, NEC Corporation, Fuchu-shi, Tokyo 183, Japan.

[1]R. P. Hamilton *et al.*, Phys. Rev. Lett. **44**, 1179 (1980).

[2]T. Tsuboyama *et al.*, Phys. Rev. D **28**, 2135 (1983), and earlier references therein.

[3]M. Bogdanski *et al.*, Phys. Lett. **62B**, 117 (1976).

[4]E. Leader, Phys. Lett. **60B**, 290 (1976).

[5]R. A. Bryan and R. J. N. Phillips, Nucl. Phys. **B5**, 201 (1968), and **B7**, 481(E) (1968).

[6]In this experiment, we concurrently measured the differential cross sections for the reactions $\bar{p}p \to \bar{p}p$, $\pi^+\pi^-$, and K^+K^-, which are being analyzed.

[7]K. Nakamura *et al.*, Phys. Rev. Lett. **52**, 731 (1984).

[8]The boundary condition model was originally proposed by O. D. Dalkarov and F. Myhrer, Nuovo Cimento, **40A**, 152 (1977). The $\bar{p}p \to \bar{n}n$ differential cross sections quoted in this Letter were calculated by T. Mizutani, F. Myhrer, and R.Tagen, private communication.

[9]J. Côté *et al.*, Phys. Rev. Lett. **48**, 1319 (1982).

[10]P. H. Timmers *et al.*, Phys. Rev. D **29**, 1928 (1984).

[11]R. A. Bryan and B. L. Scott, Phys. Rev. **177**, 1435 (1969).